FRACTURE ANALYSIS OF SINGLE AND MULTIPLE CRACK PROPAGATION IN A THERMALLY SHOCKED STRIP

H.-A. Bahr[1)], M. Kuna[2)], H.G. Maschke[2)], F. Meissner[3)], H.-J. Weiss[1)]

For an array of parallel equidistant edge cracks in a long strip, the time-dependent stress intensities due to quenching have been calculated by means of the weight function method and the boundary element method. The sequence of stages in crack pattern formation is analysed. The patterns derived theoretically are found to have essential features in common with experimental ones.

INTRODUCTION

The stress field penetrating into the thermally shocked sample provides a time-dependent energy release rate at the cracks, which can be considered as the driving force for crack propagation. It is reduced by mutual unloading of neighbouring cracks progressively with crack length. The formation of hierarchical crack patterns (Fig.1) can be regarded as a result of the opposing actions of driving force and crack interaction.

Following Stahn and Kerkhof (1), Emery and Kobayashi (2), Nemat-Nasser (3) and Bazant (4) a fracture mechanical approach for the investigation of thermal shock induced cracking was developed by Bahr and Weiss (5,6).

1) Zentralinstitut für Festkörperphysik und Werkstoffforschung, 8027 Dresden, Helmholtzstraße, DDR
2) Institut für Festkörperphysik und Elektronenmikroskopie, 4050 Halle, Weinberg 2, DDR
3) Technische Universität, Sekt. Maschinenbauelemente, 9010 Karl-Marx-Stadt, PSF 964, DDR

The consideration of time-dependent energy release rates suggested that the experimentally observed final crack patterns (Fig.1) may have developed stably from a transient state of unstable crack growth initiated from preexisting cracks.

To substantiate the previous findings, numerical calculations have been performed for a heated long strip with a single edge crack by Bahr et al. (7) or periodically arranged edge cracks as presented in this paper. The essential features of this two-dimensional problem should be transferable to more complex crack configurations.

TEMPERATURE AND STRESS FIELDS

The cracks are arranged as shown in Fig.4. They are supposed to remain straight and thus do not influence the heat flow. Therefore the heat flow problem is one-dimensional, with the solution

$$T(x,t) = -\Delta T \sum_{n=1}^{\infty} \frac{2 \sin\mu_n \cos(\mu_n x/b - \mu_n)}{\mu_n + \sin\mu_n \cos\mu_n} \exp(-\mu_n^2 \varkappa t/b^2). \tag{1}$$

The symbols b, ΔT, $\varkappa$, k, and h denote width of the strip, temperature difference in quenching, thermal diffusivity, thermal conductivity, and heat transfer coefficient, resp. The constants μ_n are the positive solutions of the equation $\mu_n = (hb/k)\cdot\cot\mu_n$. Newtonian cooling with hb/k=10 is considered. The thermal stress component $\sigma_y(x,t)$ in the absence of cracks would be

$$\sigma_y(x,t) = -E\alpha\left[T(x,t) - \frac{1}{b}\int_0^b T(x,t)\,dx - \frac{12}{b}\left(\frac{x}{b} - \frac{1}{2}\right)\int_0^b \left(\frac{x}{b} - \frac{1}{2}\right) T(x,t)\,dx\right] \tag{2}$$

with E and α denoting Young's Modulus and thermal expansion coefficient.

CALCULATION OF STRESS INTENSITY FACTORS

For any thermal loading case an equivalent face loading can be found which is equal but opposite to the tractions on the prospective crack lines in the body without cracks.

The time-dependent stress intensity factor K_I for a single crack of length "a" under Mode I loading can be determined by means of the weight function method:

$$K_I(a,t) = \sqrt{\frac{2}{\pi}} \int_0^a M(a,x)\, \sigma_y(x,t)\, dx \quad . \tag{3}$$

The weight function M(a,x) was derived by Bueckner (8) for the single edge cracked strip and has been used here in the same way as in reference (1).

Next, the boundary element analysis code ATALANTE by Maschke and Kuna (9) for solving two dimensional problems in linear elastic fracture mechanics has been applied. The program is based on the direct boundary element method (BEM), involving the free space Green's function and 3-noded elements of quadratic isoparametric shape functions. Special boundary elements were employed for modelling the crack tip. The stress intensity factor is obtained from the BEM-solution utilizing either the crack face displacements or the traction values of the crack tip node (7). By a special option of the BEM-system, periodical structures can be treated, which is essential for analyzing multiple crack configurations. Fig. 2 shows one of the BEM-discretizations used for the analysis of periodically arranged cracks of two different lengths.

CRACK PROPAGATION SCENARIO

Fig. 4 shows the normalized energy release rate plotted versus crack length. Crack propagation starts as soon as $\mathcal{G} = K_I^2/E$ exceeds a critical value $\mathcal{G}_c$ and continues as long as this condition is met. There is a critical severity of shock, ΔT_c , below which no cracking occurs. Just at $\Delta T = \Delta T_c$, single crack propagation is observed, with the crack running unstably. Excess released energy may drive the crack beyond the envelope of the family of $\mathcal{G}$-curves (solid arrow in Fig. 4).

Higher ΔT means lower $\mathcal{G}_c$-level in our normalized plot. It is seen from Fig. 4 that with increasing ΔT the delay of crack initiation after shock is diminished. As a consequence, the unstable crack paths are shorter. Furthermore, some of those initial flaws which are partly unloaded by the growing cracks may still be able to start later when their $\mathcal{G}$ increases as the cooling goes on penetrating into the strip.

This consecutive activation of initial flaws has been analyzed for a periodic array by means of BEM (Fig. 2):

By variation of the crack spacing p, the minimum spacing is found where the remaining initial flaws of length $a_2=a_0$ will just be able to start while they would not do so with lower distance. This implies 3 conditions on the energy release rates $\mathcal{G}_i$ from which a_1, t and p can be determined (i=1,2 refers to the two sets of cracks in the array):

$$\mathcal{G}_i(a_1,a_2,t,p,\Delta T) = \mathcal{G}_c \,, \tag{4}$$

$$\mathcal{G}_2 = F(a_2,t,p,\Delta T) \rightarrow \mathrm{Max} \tag{5}$$

where F follows from (4) by eliminating a_1, and Max means $\partial F/\partial t = 0$.

It is found that larger ΔT results in smaller p (see inserts in Fig.4). These conditions govern the establishment of the so-called parking order of cracks by combined unstable and stable crack propagation.

Once the parking order of cracks has been established, further propagation is governed by the penetration of cooling into depth. The law of propagation is provided by the conditions

$$a_1(t) = a_2(t) \,, \tag{6}$$

$$\mathcal{G}_i(a_1,a_2,t,p,\Delta T) = \mathcal{G}_c \,. \tag{7}$$

As a consequence of progressive mutual unloading of the growing cracks, not all of them keep propagating: There is a bifurcation-type instability with every second crack popping off while the remaining ones are left behind as in references (3,4). This occurs as soon as the following condition is fulfilled

$$\frac{\partial}{\partial a_1}\mathcal{G}_1(a_1,a_2,t,p,\Delta T) = 0 \,, \quad a_1 = a_2 \,. \tag{8}$$

The computations revealed two events of this kind for an arbitraryly chosen $\Delta T = 2.9\,\Delta T_c$ (see inserts of Fig.4).

When the crack has reached a length where its energy release rate does no more increase with time for fixed crack length, it stops. Thus the final crack length and the time of crack stop are determined by the conditions

$$\mathcal{G}_i(a_1,a_2,t,p,\Delta T) = \mathcal{G}_c \,, \quad a_1 = a_2 \,, \tag{9}$$

$$\frac{\partial}{\partial t}\mathcal{G}_i(a_1,a_2,t,p,\Delta T) = 0 \,, \quad a_1 = a_2 \,. \tag{10}$$

For $\Delta T = 1.6\,\Delta T_c$ one obtains a/b=0.254. More severe shock leads to larger final crack lengths (Fig.4).

Note that the envelope of the multiple crack $\mathcal{G}$-curves differs from that of the single crack $\mathcal{G}$-curves. The calculated final crack lengths turned out to depend non-monotonically on ΔT. This is compatible with the non-monotonic dependence of retained strength on ΔT as found in reference (10) (Fig.3).

The numerical results obtained for the quenched edge cracked strip support the fracture mechanical approach to thermal shock damage of brittle materials due to single and multiple crack growth recently proposed in references (5,6). It allows to draw quantitative conclusions concerning the dependence of damage on severity of shock, initial strength and heat transfer.

REFERENCES

(1) Stahn, D. and Kerkhof, F., Glastechn. Berichte, Vol.50, 1977, pp.121-128.

(2) Emery, A.F. and Kobayashi, A.S., J.Amer.Ceram.Soc., Vol.63, 1980, pp.410-415.

(3) Nemat-Nasser, S., Keer, L.M. and Parihar, K.S., Int.J.Solids Struct., Vol.14, 1978, pp.409-430.

(4) Bazant, Z.P., Ohtsubo, H. and Ach, K., Internat.J.Fracture, Vol.15, 1979, pp.443-456.

(5) Bahr, H.-A. and Weiss, H.-J., Theoret.Appl.Fracture Mech., Vol.6, 1986, pp.57-62.

(6) Bahr, H.-A., Fischer, G. and H.-J. Weiss, J.Mater.Sci., Vol.21, 1986, pp.2716-2720.

(7) Bahr, H.-A., Balke, H., Kuna, M. and Liesk, H., Theoret.Appl.Fracture Mech., Vol.8, 1987, pp.33-39.

(8) Bueckner, H.F., ZAMM, Vol.51, 1971, pp.97-109.

(9) Maschke, H.G. and Kuna, M., Theoret.Appl.Fracture Mech., Vol.4, 1985, pp.181-189.

(10) Bertsch, B.E., Larson, D.R. and Hasselman, D.P.H., J.Amer.Ceram.Soc., Vol.57, 1974, pp.235-236.

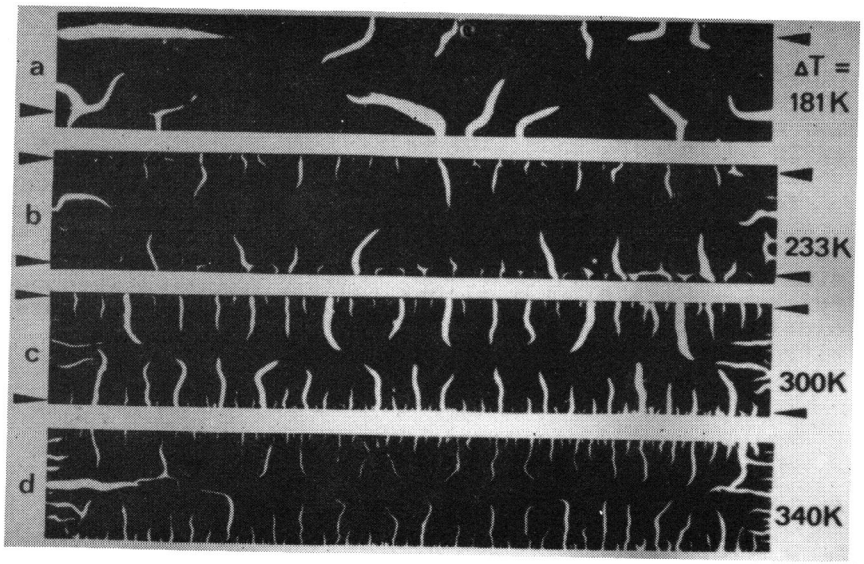

Figure 1 Crack penetration patterns in quenched glass-ceramic slabs. Curtesy by G. Fischer.

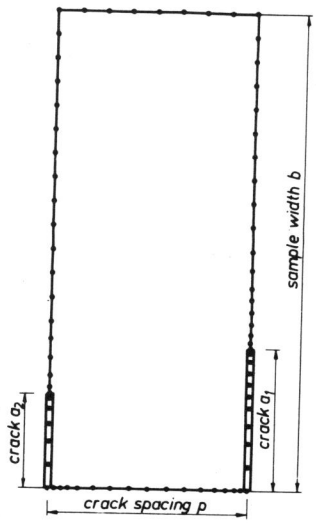

Figure 2 Boundary element mesh

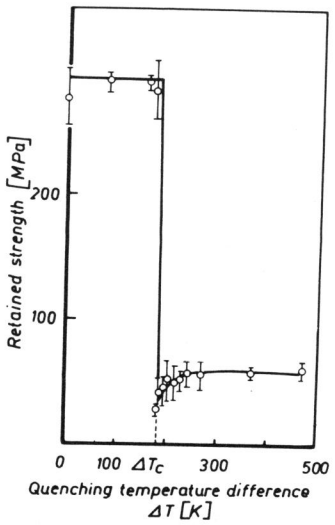

Figure 3 Thermal shock data after reference (10)

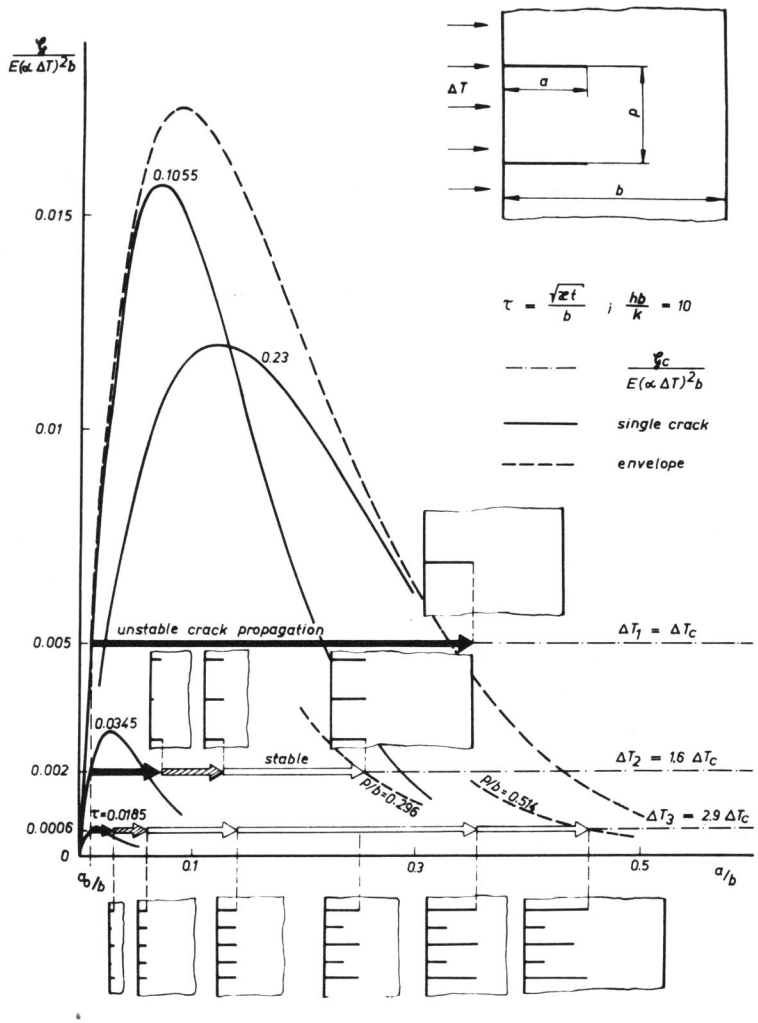

Inserts representing numerical results

Figure 4 Crack propagation scenario derived from time-dependent energy release rate $\mathcal{G}$ for several ΔT